PHYSICAL REVIEW B **87**, 041306(R) (2013)

Strong optical polarization in nonpolar ($1\bar{1}00$) $Al_xGa_{1-x}N$/AlN quantum wells

Mitsuru Funato,[*] Kazuhisa Matsuda, Ryan G. Banal, Ryota Ishii, and Yoichi Kawakami[†]
Department of Electronic Science and Engineering, Kyoto University, Kyoto 615-8510, Japan
(Received 16 November 2012; revised manuscript received 7 January 2013; published 25 January 2013)

The optical polarization properties in nonpolar ($1\bar{1}00$) $Al_xGa_{1-x}N$/AlN quantum wells (QWs) are investigated over the full range of Al compositions. The $\boldsymbol{k}\cdot\boldsymbol{p}$ calculation predicts that the lowest energy optical transition in ($1\bar{1}00$) $Al_xGa_{1-x}N$ layers pseudomorphically grown on unstrained AlN is dipole allowed for the electric field vector parallel to the [0001] direction, and that the degree of polarization is hardly affected by the $Al_xGa_{1-x}N$ QW width regardless of the Al composition. Experimentally, $Al_xGa_{1-x}N$/AlN QWs ($0 \leqslant x \leqslant 0.81$) are homoepitaxially grown on AlN substrates. Photoluminescence spectroscopy reveals that the emissions of all QWs, including GaN/AlN QWs, are strongly polarized along the [0001] direction. This result agrees with the theoretical prediction.

DOI: 10.1103/PhysRevB.87.041306 PACS number(s): 78.67.De, 78.55.Cr, 73.21.Fg, 81.07.St

Deep-ultraviolet (DUV) light sources such as Hg lamps and excimer lasers have some significant disadvantages, including low energy conversion efficiency and harmful constituents. Hence, there has been increased social pressure to replace them. To this end, $Al_xGa_{1-x}N$ quantum wells (QWs) show promise, and are the subjects of extensive studies.[1–3] This is because $Al_xGa_{1-x}N$ is a harmless III-nitride semiconductor alloy composed of binary GaN and AlN with an Al composition of x, and has a direct band gap that can be tuned for the DUV spectral region. For optoelectronic applications, understanding the $Al_xGa_{1-x}N$ band structures and the optical properties is crucial, for which numerous factors such as GaN and AlN band structures as well as strain and quantum confinement within $Al_xGa_{1-x}N$ QW emitters have to be considered.

Wurtzite AlN and GaN exhibit three distinct valence bands at the Brillouin zone center because the degeneracy of the p-like states at the Γ point is lifted by both crystal-field splitting and spin-orbit splitting. Interestingly, the crystal-field splitting energy (Δ_1) of AlN is negative,[4–8] whereas Δ_1 of GaN is positive. Consequently, the topmost valence band in AlN is the crystal-field splitoff hole band governed by the p_z-like state, while that in GaN is the heavy hole band governed by the p_x-like and p_y-like states. Here, orthogonal coordinates x and y are in the (0001) plane, while z is normal to it. Due to this difference in the valence-band structures, optical polarization may switch between GaN-like $\boldsymbol{E} \perp [0001]$ and AlN-like $\boldsymbol{E} \parallel [0001]$ at a certain Al composition,[9,10] where $\boldsymbol{E}$ is the electric field vector of emitted light.

It is noteworthy that the critical Al composition for polarization switching strongly depends on both strain and quantum confinement.[9,10] For coherent $Al_xGa_{1-x}N$ layers on unstrained AlN with a conventional (0001) interface, the polarization switches at $x \sim 0.6$. This characteristic suggests a weak surface emission from c-oriented Al-rich $Al_xGa_{1-x}N$. Although the use of thin $Al_xGa_{1-x}N$ QWs has been demonstrated to enhance the surface emission,[9,10] the critical Al composition remains $x \sim 0.8$. As theoretically predicted,[11,12] a promising alternative to achieve a strong surface emission from Al-rich $Al_xGa_{1-x}N$ QWs is growth on non-c planes such as ($1\bar{1}00$) and ($11\bar{2}2$). Additionally, the non-c plane may provide another benefit, low threshold carrier densities for lasing operation.[13,14] However, the theoretical predictions rely on physical parameters that have yet to be determined unambiguously. Furthermore, although growth of $Al_xGa_{1-x}N$ films has been reported,[15] detailed optical properties of non-c plane $Al_xGa_{1-x}N$/AlN QWs have yet to be experimentally investigated. Herein, we theoretically assess the band structures and related band-to-band transitions in nonpolar $Al_xGa_{1-x}N$/AlN QWs using the $\boldsymbol{k}\cdot\boldsymbol{p}$ method and the latest physical parameters. Additionally, we experimentally demonstrate a strong optical anisotropy in $Al_xGa_{1-x}N$/AlN QWs homoepitaxially grown on ($1\bar{1}00$) m plane AlN substrates.

We used the six-band $\boldsymbol{k}\cdot\boldsymbol{p}$ theory exclusive of the excitonic effect for the calculation.[16,17] To predict optical properties more precisely, not the simple band-to-band picture but the excitonic picture should be adopted. The general theory involving the excitonic effect has already been established,[18] and used for GaN.[19–21] Particularly in Ref. 19, the optical anisotropy of excitons in strained ($1\bar{1}00$) GaN has been discussed, and the important elements to determine the anisotropy have been clarified. For AlN, on the other hand, the band structure is markedly different from that of GaN, and the material parameters are less reliable. For example, the spin-exchange interaction constant describing the energy splitting between the spin-singlet and triplet terms remains controversial, which hampers including the excitonic effect into analyses. However, we demonstrate in this study that the band-to-band picture based on the six-band $\boldsymbol{k}\cdot\boldsymbol{p}$ theory well approximates the experimentally revealed optical anisotropy in ($1\bar{1}00$) $Al_xGa_{1-x}N$/AlN QWs.

Table I lists the parameters. We recently determined all the deformation potentials (C_i, i = 1–6) in GaN (Ref. 21) and the hydrostatic deformation potentials (C_1 and C_2) in AlN,[23] and found the definite breakdown of the conventionally well-adopted quasicubic approximation. To determine the deformation potentials, the appropriate set of the elastic constants was selected for each material. For strain, we considered an out-of-plane component along the [$1\bar{1}00$] growth direction (ϵ_{xx}) and in-plane components along the [$11\bar{2}0$] direction [$\epsilon_{yy} = (a_0 - a)/a$] and the [0001] direction [$\epsilon_{zz} = (c_0 - c)/c$], but ignored the remaining shear components, referring to the classical elasticity theory.[27] Here, a and c are the unstrained lattice parameters, while the subscript 0 means

 ©2013 American Physical Society

TABLE I. Physical parameters used in the calculation.

		AlN	GaN
Lattice parameter (nm)[a]	c	0.4982	0.5185
	a	0.3112	0.3189
Crystal-field interaction (meV)	Δ_1	-212[b]	12.3[c]
Spin-orbit interaction $\parallel c$ (meV)	Δ_2	5.3[b]	5.2[c]
Spin-orbit interaction $\perp c$ (meV)	Δ_3	5.3[b]	5.9[c]
Deformation potential (eV)	C_1	4.3[d]	6.5[c]
	C_2	11.5[d]	11.2[c]
	C_3	9.22[e]	4.9[c]
	C_4	-3.74[e]	-5.0[c]
	C_5	-3.30[e]	-2.8[c]
Elastic stiffness constant (GPa)	c_{11}	394[f]	373[g]
	c_{12}	134[f]	141[g]
	c_{13}	95[f]	80[g]
	c_{33}	402[f]	387[g]
	c_{44}	121[f]	94[g]
Valence-band parameter[a]	A_1	-3.86	-7.21
	A_2	-0.25	-0.44
	A_3	3.58	6.68
	A_4	-1.32	-3.46
	A_5	-1.47	-3.40

[a]Reference 22.
[b]Reference 8.
[c]Reference 21.
[d]Reference 23.
[e]Reference 24.
[f]Reference 25.
[g]Reference 26.

those under strain. The strain components have a relationship of $\epsilon_{xx} = -(c_{12}\epsilon_{yy} + c_{13}\epsilon_{zz})/c_{11}$, where c_{ij}'s are the elastic stiffness constants.

Figure 1 displays the calculated valence-band energies in $(1\bar{1}00)$ $Al_xGa_{1-x}N$ single layers pseudomorphically grown on unstrained AlN. A, B, and C denote the three valence bands in the order of low to high hole energies. In AlN, the A band is mainly composed of the p_z-like state, and that band is always topmost in $Al_xGa_{1-x}N$ $(0 \leqslant x \leqslant 1)$ without band crossing or anticrossing. Therefore, it is deduced that the lowest energy transition between the conduction and valence bands in pseudomorphic $(1\bar{1}00)$ $Al_xGa_{1-x}N$ on AlN is related to the p_z-like state and is polarized along the [0001] direction. Because the [0001] direction is within the $(1\bar{1}00)$ plane, the calculation predicts a strongly anisotropic in-plane polarization of the emission from $(1\bar{1}00)$ $Al_xGa_{1-x}N$ on AlN.

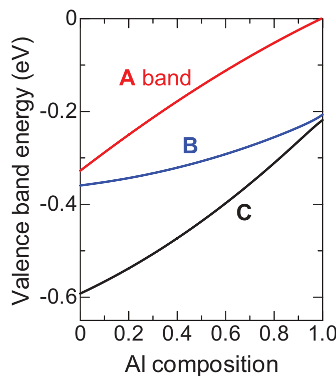

FIG. 1. (Color online) Calculated A, B, and C valence-band energies in pseudomorphic $(1\bar{1}00)$ $Al_xGa_{1-x}N$ single layers on unstrained AlN as functions of Al composition. Relative energies with respect to the A valence band in AlN are drawn.

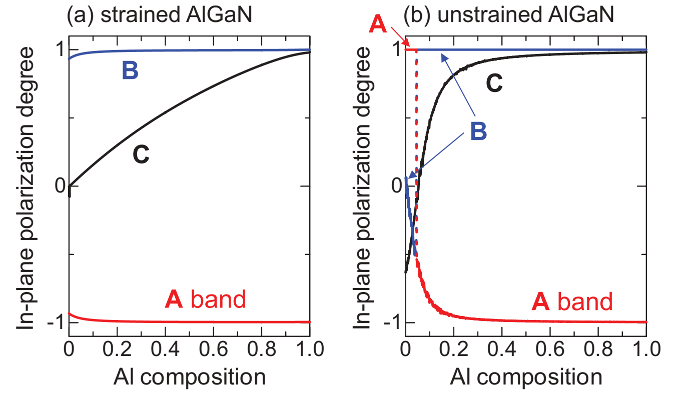

FIG. 2. (Color online) In-plane polarization degrees concerning A, B, and C band-related transitions in (a) pseudomorphic and (b) strain-relaxed $(1\bar{1}00)$ $Al_xGa_{1-x}N$ single layers on AlN.

Figure 2 indicates the calculated degrees of the in-plane polarizations of the A, B, and C band-related transitions in $(1\bar{1}00)$ $Al_xGa_{1-x}N/AlN$, where the polarization degree (ρ) is defined as $(M_\perp^2 - M_\parallel^2)/(M_\perp^2 + M_\parallel^2)$ using the matrix elements perpendicular ($M_\perp$) and parallel ($M_\parallel$) to the [0001] axis. Figures 2(a) and 2(b) compare the polarization degrees for pseudomorphic and strain-relaxed $(1\bar{1}00)$ $Al_xGa_{1-x}N$ single layers on unstrained AlN, respectively. In pseudomorphic $Al_xGa_{1-x}N$, the A band-related transition is polarized almost linearly along the [0001] direction ($\rho \sim -1$) for all Al compositions. On the other hand, strain relaxation causes polarization switching between GaN-like $\boldsymbol{E} \perp [0001]$ ($\rho > 0$) and AlN-like $\boldsymbol{E} \parallel [0001]$ ($\rho < 0$) at $x \sim 0.045$ due to the emergence of the GaN-like nature with a low Al content AlGaN.

In practical light emitting applications, QWs are essential structures. Thus, the quantum confinement effect on the in-plane polarization properties was calculated for the A band-related transition with an assumed structure of pseudomorphic $Al_xGa_{1-x}N/AlN$ QWs on unstrained AlN underlying layers. Figure 3(a) shows the calculated results for well widths of 1, 2, 5, and 10 nm. The polarization degree is almost independent of the well width as long as the pseudomorphic growth is preserved, and the calculated results cannot be well resolved. It is noteworthy that the GaN QWs in Ref. 28, which have an infinite barrier height, may exhibit polarization switching as the well width decreases. In contrast, our calculation for GaN/AlN QWs does not indicate such a switching behavior [Fig. 3(a)]. This discrepancy is due to the material parameters used in the calculations, as already noted in Ref. 28. An experimental demonstration of the polarization degree is indispensable to reach a conclusion.

To qualitatively understand the cause of the well-width insensitive polarization degree, we calculated the effective hole mass along the $[1\bar{1}00]$ growth direction for each valence band within the framework of the $\boldsymbol{k} \cdot \boldsymbol{p}$ theory, where the strain due to the lattice mismatch with the unstrained AlN

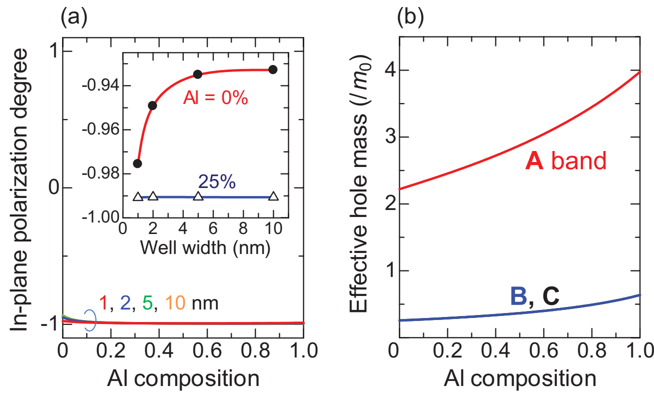

FIG. 3. (Color online) (a) In-plane polarization degree of the A band-related transition in pseudomorphic ($1\bar{1}00$) $Al_xGa_{1-x}N$/AlN QWs on unstrained AlN. Assumed well widths are 1, 2, 5, and 10 nm. The inset indicates the in-plane polarization degree as a function of well width for GaN/AlN and $Al_{0.25}Ga_{0.75}N$/AlN QWs. Very small variation is confirmed. (b) Calculated effective hole masses along the [$1\bar{1}00$] direction ($\perp$[0001]) for the A, B, and C bands in the unit of the electron mass (m_0). The strain within the ($1\bar{1}00$) plane due to the lattice mismatch with the unstrained AlN underlying layer is taken into account.

underlying layer is considered.[16] The results are shown in Fig. 3(b). The A valence band has a heavier hole mass than the B and C bands, while B and C bands possess similar hole masses for all Al compositions. Therefore, the valence-band order is not affected by quantum confinement, which is why the polarization degree is rather insensitive to it. Note that the properties demonstrated in Fig. 3 are for pseudomorphic $Al_xGa_{1-x}N$/AlN QWs on unstrained AlN underlying layers, whereas strain relaxation in the QWs may cause polarization switching as suggested in Fig. 2.

For crystal growth of nonpolar ($1\bar{1}00$) $Al_xGa_{1-x}N$ QWs, we used (0001) AlN substrates prepared by the physical vapor transport method. To obtain fresh ($1\bar{1}00$) surfaces, the (0001) substrates were cleaved at the ($1\bar{1}00$) plane in air, as illustrated in Fig. 4. Atomic force microscopy revealed that the cleaved ($1\bar{1}00$) surface is atomically smooth with a root-mean-square (rms) roughness of 0.7 nm. Immediately after cleavage, the substrate was loaded into a reactor for metalorganic vapor phase epitaxy (MOVPE). Then the substrate was heated to the growth temperature under an NH_3 atmosphere. The source precursors, trimethylaluminum, trimethygallium, and NH_3,

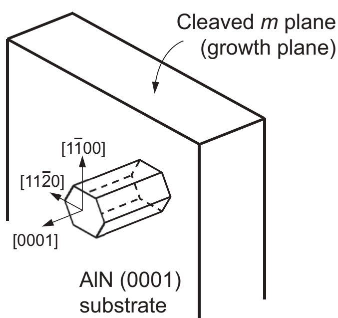

FIG. 4. Configuration of the crystal axes of the AlN substrate.

TABLE II. Fabricated ($1\bar{1}00$) $Al_xGa_{1-x}N$/AlN QWs.

Al (%)	0	0	0	19	35	56	58	60	61	81
QW width (nm)	0.5	0.8	1.0	3.8	3.8	6.5	3.8	3.8	6.5	3.8
QW periods	1	1	1	1	2	5	3	3	5	5

were supplied continuously without growth interruption. The samples were not intentionally doped with impurities.

Initially, we employed the MOVPE growth conditions established for (0001) AlN, which are a growth temperature of 1200 °C, a reactor pressure of 76 Torr, and a V/III ratio of 174.[29,30] However, the resulting surface had an rms roughness value as high as 37.7 nm. We examined several different substrates, including commercially available ($1\bar{1}00$) AlN substrates, but a significant difference was not observed. Therefore, we optimized the growth conditions. To date, the best surface has been achieved by the following procedure: growth of ~350-nm-thick AlN at 1050 °C with a pressure of 38 Torr and a V/III ratio of 1300, followed by ~600-nm-thick AlN growth at 1200 °C without changing the remaining parameters. These conditions reduce the surface rms roughness to 7.6 nm. Although surface undulations remain, their angles with respect to the ($1\bar{1}00$) plane are within 10° and do not affect the polarization properties; this assertion is theoretically confirmed by the $\boldsymbol{k} \cdot \boldsymbol{p}$ method. The x-ray linewidths for symmetric ($1\bar{1}00$) and asymmetric ($1\bar{1}02$) diffractions are identical before and after epitaxy. Furthermore, photoluminescence (PL) at 10 K is dominated by an emission due to donor-bound excitons, indicating suitable optical properties.

$Al_xGa_{1-x}N$/AlN QWs were fabricated on the optimized ($1\bar{1}00$) AlN. The AlN barriers are 22.5 nm thick, while the $Al_xGa_{1-x}N$ well widths vary (Table II). Because the Al compositions are estimated from the PL emission energy, they might be underestimated due to exciton or carrier localization at potential minima. However, this is the best effort for single QWs because x-ray diffraction barely provides information on their QW parameters.

PL spectroscopy at 10 K was used to assess the optical properties. The excitation source was a pulsed ArF excimer laser (193 nm) with a repetition frequency of 25 Hz and a pulse duration of 4 ns. The typical excitation power density was 4 MW/cm^2. The spectra were acquired by a 50-cm monochromator in conjunction with a liquid-N_2-cooled CCD camera (resolution: 0.045 nm). The system polarization was calibrated for all PL spectra. Figure 5(a) displays the PL spectra of nonpolar ($1\bar{1}00$) $Al_xGa_{1-x}N$/AlN QWs, and clearly demonstrates that the emission energy can be tuned through band-gap engineering based on the Al composition and well width.

Before discussing the in-plane polarization, the out-of-plane polarization was assessed by collecting PL from the ($11\bar{2}0$) plane of the sample edge. (See Fig. 4.) Placing a linear polarizer after the collimating lens confirmed that the out-of-plane component ($\boldsymbol{E} \perp c$, i.e., $\boldsymbol{E} \parallel [1\bar{1}00]$) of the emission is much weaker than the in-plane component ($\boldsymbol{E} \parallel c$), as suggested theoretically in Fig. 1. Then the PL setup was modified; the incident angle of the laser was changed to 60° from the surface normal, and PL was collected at the surface

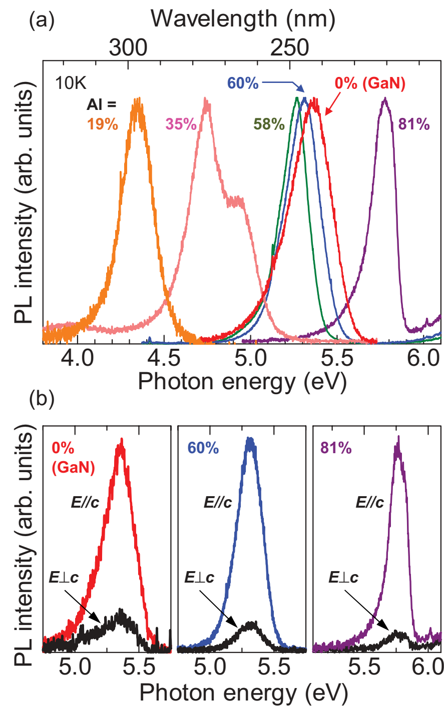

FIG. 5. (Color online) (a) PL spectra of nonpolar $(1\bar{1}00)$ $Al_xGa_{1-x}N$/AlN QWs at 10 K. The well width of GaN QW is 0.5 nm, while those for the remaining QWs are 3.8 nm. (b) In-plane polarization PL spectra for select QWs.

normal. This configuration allowed the in-plane polarization PL properties of $\boldsymbol{E} \perp c$ and $\boldsymbol{E} \parallel c$ to be directly assessed using a linear polarizer inserted after a collimating lens.

Figure 5(b) shows examples of the in-plane polarization PL spectra. For all Al compositions ($x = 0$, 60%, and 81%), the observed trends are similar; all the samples, including a GaN single QW, show $\boldsymbol{E} \parallel [0001]$ polarization. To survey the in-plane polarization properties, Fig. 6 plots the polarization degrees, where the calculated results for pseudomorphic and unstrained layers are also drawn. The experimental

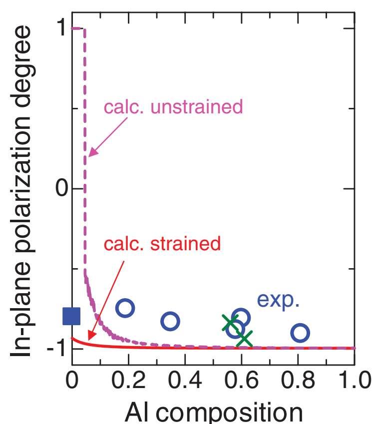

FIG. 6. (Color online) In-plane polarization degree of nonpolar $(1\bar{1}00)$ $Al_xGa_{1-x}N$/AlN QWs. Squares, circles, and crosses represent QWs with thicknesses of 0.5, 3.8, and 6.5 nm, respectively. Curves are the calculated polarization degrees for pseudomorphic and unstrained QWs.

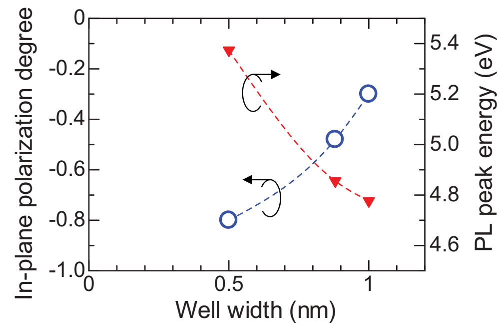

FIG. 7. (Color online) Polarization degree and emission energy of GaN/AlN single QWs with various well widths.

polarization degrees range from −0.75 to −0.95, indicating a strong $\boldsymbol{E} \parallel [0001]$ polarization. Furthermore, the Al composition and well width negligibly influence the polarization degree, which agrees well with our calculations for pseudomorphic QWs. Hence, we conclude that all the samples shown in Fig. 6 are pseudomorphic, and strain but not quantum confinement is responsible for the valence-band ordering and the consequent polarization in nonpolar pseudomorphic AlGaN/AlN QWs.

As shown in Figs. 2 and 6, strain relaxation causes polarization switching in the AlGaN/AlN system with Al compositions less than 0.045. Experimentally, to ensure the pseudomorphic growth, the thinnest (0.5 nm) QW was used for the GaN/AlN system in Fig. 6. [Although it is difficult to predict the critical layer thickness in $(1\bar{1}00)$ AlGaN/AlN due to the lack of knowledge on the lattice relaxation mechanism, we estimate it to be 2.4 nm for $(1\bar{1}00)$ GaN on AlN,[31] assuming the same relaxation mechanism as in $(1\bar{1}00)$ InGaN/GaN.[32]] As mentioned above, on the other hand, a different set of material parameters has predicted that polarization switching may occur even in pseudomorphic GaN/AlN QWs due to GaN QW thickness.[28] That is, two different effects may superimpose each other in GaN/AlN QWs. To clarify this issue, we experimentally investigated the dependence of the polarization degree on GaN well thickness. Figure 7 demonstrates that thinner GaN QWs promote $\boldsymbol{E} \parallel [0001]$ polarization, and decreasing the well width down to 0.5 nm does not switch $\boldsymbol{E} \parallel [0001]$ to $\boldsymbol{E} \perp [0001]$. The observed nonswitching behavior contradicts the theoretical prediction in Ref. 28. On the other hand, our calculations (Figs. 2, 3, and 6) indicate that the in-plane polarization is independent of well width for pseudomorphic $Al_xGa_{1-x}N$ and that lattice relaxation promotes the $\boldsymbol{E} \perp [0001]$ polarization. Therefore, the experimental observations in Fig. 7 are most likely due to the progress of lattice relaxation, and the polarization switching does not occur within the experimental limit.

It is interesting to discuss the reason for the difference between Ref. 28 and our study. Reference 28 presents an analytical equation for polarization switching, which suggests that the sign of $A_4 - A_5$ for a QW material essentially determines the well-width dependence of the polarization property. (A's are the valence-band effective-mass parameters listed in Table I.) Their A_4 and A_5 for GaN are −2.83 and −3.13, respectively, whereas ours are −3.46 and −3.40. In

fact, the signs of $A_4 - A_5$ in this work and Ref. 28 have opposite signs, and may explain why the polarization is sensitive to well width in Ref. 28, but insensitive herein. In turn, the experimental data depicted in Fig. 6 strongly suggest that $A_4 < A_5$ could be satisfied in GaN, although the exact values remain controversial.

*funato@kuee.kyoto-u.ac.jp
†kawakami@kuee.kyoto-u.ac.jp

[1] H. Hirayama, J. Appl. Phys. **97**, 091101 (2005).
[2] A. Khan, K. Balakrishnan, and T. Katona, Nat. Photonics **2**, 77 (2008).
[3] T. Oto, R. G. Banal, K. Kataoka, M. Funato, and Y. Kawakami, Nat. Photonics **4**, 767 (2010).
[4] M. Suzuki, T. Uenoyama, and A. Yanase, Phys. Rev. B **52**, 8132 (1995).
[5] S.-H. Wei and A. Zunger, Appl. Phys. Lett. **69**, 2719 (1996).
[6] J. Li, K. B. Nam, M. L. Nakarmi, J. Y. Lin, H. X. Jiang, P. Carrier, and S.-H. Wei, Appl. Phys. Lett. **83**, 5163 (2003).
[7] E. Silveira, J. A. Freitas, Jr., O. J. Glembocki, G. A. Slack, and L. J. Schowalter, Phys. Rev. B **71**, 041201(R) (2005).
[8] G. Rossbach, M. Feneberg, M. Röppischer, C. Werner, N. Esser, C. Cobet, T. Meisch, K. Thonke, A. Dadgar, J. Blasing, A. Krost, and R. Goldhahn, Phys. Rev. B **83**, 195202 (2011).
[9] A. A. Yamaguchi, Phys. Status Solidi C **5**, 2364 (2008).
[10] R. G. Banal, M. Funato, and Y. Kawakami, Phys. Rev. B **79**, 121308(R) (2009).
[11] J. Bhattacharyya, S. Ghosh, and H. T. Grahn, Phys. Status Solidi B **246**, 1184 (2009).
[12] A. A. Yamaguchi, Appl. Phys. Lett. **96**, 151911 (2010).
[13] K. Kojima, A. A. Yamaguchi, M. Funato, Y. Kawakami, and S. Noda, J. Appl. Phys. **110**, 043115 (2011).
[14] S.-H. Park, J. Appl. Phys. **110**, 063105 (2011).
[15] M. R. Laskar, T. Ganguli, A. A. Rahman, A. P. Shah, M. R. Gokhale, and A. Bhattacharya, Phys. Status Solidi RRL **4**, 163 (2010).
[16] S. L. Chuang and C. S. Chang, Phys. Rev. B **54**, 2491 (1996).
[17] S.-H. Park and S. L. Chuang, Phys. Rev. B **59**, 4725 (1999).
[18] G. L. Bir and G. E. Pikus, *Symmetry and Strain-Induced Effects in Semiconductors* (Wiley, New York, 1974).
[19] B. Gil and A. Alemu, Phys. Rev. B **56**, 12446 (1997).
[20] M. Julier, J. Campo, B. Gil, J. P. Lascaray, and S. Nakamura, Phys. Rev. B **57**, R6791 (1998).
[21] R. Ishii, A. Kaneta, M. Funato, Y. Kawakami, and A. A. Yamaguchi, Phys. Rev. B **81**, 155202 (2010).
[22] I. Vurgaftman and J. R. Meyer, J. Appl. Phys. **94**, 3675 (2003).
[23] R. Ishii, A. Kaneta, M. Funato, and Y. Kawakami (unpublished).
[24] Q. Yan, P. Rinke, M. Winkelnkemper, A. Qteish, D. Bimberg, M. Scheffler, and C. G. Van de Walle, Semicond. Sci. Technol. **26**, 014037 (2011).
[25] M. Kazan, E. Moussaed, R. Nader, and P. Masri, Phys. Status Solidi C **4**, 204 (2007).
[26] M. Yamaguchi, T. Yagi, T. Sota, T. Deguchi, K. Shimada, and S. Nakamura, J. Appl. Phys. **85**, 8502 (1999).
[27] J. F. Nye, *Physical Properties of Crystals* (Oxford Science, New York, 1957).
[28] A. A. Yamaguchi, Jpn. J. Appl. Phys. **46**, L789 (2007).
[29] R. G. Banal, M. Funato, and Y. Kawakami, J. Cryst. Growth **311**, 2834 (2009).
[30] M. Funato, K. Matsuda, R. Banal, R. Ishii, and Y. Kawakami, Appl. Phys. Express **5**, 082001 (2012).
[31] J. Nishinaka, M. Funato, and Y. Kawakami, J. Appl. Phys. **112**, 033513 (2012).
[32] S. Yoshida, T. Yokogawa, Y. Imai, S. Kimura, and O. Sakata, Appl. Phys. Lett. **99**, 131909 (2011).